

Knotting probability of DNA molecules confined in restricted volumes: DNA knotting in phage capsids

Javier Arsuaga*[†], Mariel Vázquez*, Sonia Trigueros[‡], De Witt Summers[§], and Joaquim Roca*[¶]

Departments of *Mathematics and [†]Molecular and Cell Biology, University of California, Berkeley, CA 94720; [‡]Institut de Biologia Molecular de Barcelona–Consejo Superior de Investigaciones Científicas, Jordi Girona 18–26, 08034 Barcelona, Spain; and [§]Mathematics Department, Florida State University, Tallahassee, FL 32306

Communicated by James C. Wang, Harvard University, Cambridge, MA, February 15, 2002 (received for review January 11, 2002)

When linear double-stranded DNA is packed inside bacteriophage capsids, it becomes highly compacted. However, the phage is believed to be fully effective only if the DNA is not entangled. Nevertheless, when DNA is extracted from a tailless mutant of the P4 phage, DNA is found to be cyclic and knotted (probability of 0.95). The knot spectrum is very complex, and most of the knots have a large number of crossings. We quantified the frequency and crossing numbers of these knots and concluded that, for the P4 tailless mutant, at least half the knotted molecules are formed while the DNA is still inside the viral capsid rather than during extraction. To analyze the origin of the knots formed inside the capsid, we compared our experimental results to Monte Carlo simulations of random knotting of equilateral polygons in confined volumes. These simulations showed that confinement of closed chains to tightly restricted volumes results in high knotting probabilities and the formation of knots with large crossing numbers. We conclude that the formation of the knots inside the viral capsid is driven mainly by the effects of confinement.

Knots and links are of biological interest because they preserve topological information. In particular, knotted DNA molecules can be well characterized experimentally and therefore used as assays for different biochemical reactions. Characterization of knotted products formed by random cyclization of linear molecules has been used to quantify important biochemical properties of DNA such as its effective diameter (1, 2). DNA knots and catenates obtained as the product of site-specific recombination have also been a key to unveiling the mechanism of enzymatic action (3, 4). In both cases, the development of mathematical and computational tools has helped the analysis of the experimental results greatly (5–8).

Significant numbers of DNA knots are found also in biological systems: in *Escherichia coli* cells harboring mutations in the *GyrB* or *GyrA* genes (9), bacteriophages P2 and P4 (10, 11), and cauliflower mosaic viruses (12). However, very little information about these systems has been inferred from the observed knots. In particular, interpretation of the experimental results for bacteriophages has been limited by the experimental difficulty in quantifying the complex spectrum of knotted products. These difficulties have paralleled those encountered in developing a theory for random knotting of ideal polymeric chains in cases where interactions with other macromolecules and/or confinement in small volumes have a significant function (13–15).

P4 is an icosahedral bacteriophage, the morphogenesis of which depends on the P2 helper prophage (16). The P4 genome is an 11.6-kb DNA molecule with 19-bp cohesive ends (17). During phage morphogenesis, once a proteinic procapsid is formed, one copy of the viral genome enters it. This is an ATP-consuming process carried out by the protein complex known as connector (18). In the “mature” P4 phages (i.e., complete infective particles with capsid and tail), one of the two cohesive ends of the DNA is known to remain anchored near the connector region (19), while the bulk of packed DNA plus its associated water molecules virtually occupy the total volume of the capsid (20). Despite the system’s apparent simplicity, the

overall arrangement of the DNA inside the viral capsid remains largely unknown (21–25).

Most DNA molecules extracted from P4 phages are circles that result from the cohesive-end joining of the viral genome. Previous studies have shown that such circles have a knotting probability of ≈ 0.20 when DNA is extracted from mature P4 phages (10). This high value is increased more than 4-fold when DNA is extracted from incomplete P4 phage particles (which we refer to as “capsids”) or from noninfective P4 mutants that lack the phage tail (which we refer to as “tailless mutants”; ref. 10). Knotting of DNA in P4 deletion mutants is even greater. The larger the P4 genome deletion, the higher the knotting probability (26). For P4 *vir1 del22*, containing P4’s largest known deletion (1.6 kb deleted; ref. 27), knotting probability is more than 0.80 (28). These values contrast with the knotting probability of 0.03 observed when P4 DNA molecules undergo cyclization in free solution (1, 29). These differences are still more striking when the variance in distribution of knot complexity is included. Although knots formed by random cyclization of 10-kb linear DNA in free solution have an average crossing number of less than five (1, 29), knots from phage particles have a knotting probability of 0.95 and appear to have very large crossing numbers on average (10, 26, 28).

In this paper we investigate the reasons for the high knotting probability and knot complexity of bacteriophage DNA. We measure the knotting probability and distribution of knotted molecules for P4 *vir1 del22* mature phages, capsids, and tailless mutants. We also study by Monte Carlo simulations the effects that the confinement of DNA molecules inside small volumes have on knotting probability and complexity. We conclude from our results that for tailless mutants a significant amount of DNA knots must be formed before the disruption of the phage particle, with both increased knotting probability and knot complexity driven by confinement of the DNA inside the capsid.

Materials and Methods

Bacteriophages and Bacterial Strains. Bacteriophage P4 *vir1 del22* and the *E. coli* strains C-1895 and C-8001 were provided by Richard Calendar (University of California, Berkeley, CA). P4 *vir1 del22* contains the largest known P4 deletion (27). *E. coli* C-1895 is lysogenic for P2, the helper prophage, and is used to grow stocks of P4 *vir1 del22*, from which mature phages and capsids are obtained. *E. coli* C-8001 is lysogenic for P2 *amH13*. As gene *H* encodes part of the phage tail, this strain is used to obtain tailless mutants of P4 *vir1 del22*.

Isolation of Knotted DNA from P4 Phage Particles. Knotted DNA was prepared from different P4 *vir1 del22* phage particles by following the procedure described by Isaksen *et al.* (28) with the following modifications: after bacterial lysis, phage particles

[†]To whom reprint requests should be addressed. E-mail: jrbbmc@cid.csic.es.

The publication costs of this article were defrayed in part by page charge payment. This article must therefore be hereby marked “advertisement” in accordance with 18 U.S.C. §1734 solely to indicate this fact.

were precipitated with polyethylene glycol 8000. Pancreatic DNase I incubation of phage precipitates was either omitted or extended to 5 min at 37°C. Phage precipitates were dissolved in phage buffer containing 10 mM MgCl₂, 10 mM Tris·HCl, pH 7.2, and 130 mM ammonium acetate. Mature phages and capsids (obtained from lysates of the strain C-1895) and P4 tailless mutants (obtained from lysates of the strain C-8001) were banded by cesium chloride centrifugation in an NVT65 rotor for 14 h at 45,000 rpm. The banded particles were dialyzed against phage buffer, and DNA was extracted twice with phenol and once with phenol/chloroform. In some experiments, EDTA to 25 mM or SDS to 0.5% was added to the phage particles before phenol extraction of the DNA.

Unknotting of DNA by Yeast Topoisomerase II. Yeast DNA topoisomerase II was purified from *Saccharomyces cerevisiae* strain BCY123 harboring a yeast DNA topoisomerase II expression clone YEpTOP2GAL1 as described (30). DNA was unknotted in 50- μ l reaction volumes containing 50 mM Tris·HCl, pH 8, 1 mM EDTA, 150 mM KCl, 8 mM MgCl₂, 7 mM 2-mercaptoethanol, 100 μ g/ml BSA, 5 μ g of purified phage DNA, and 50 ng of topoisomerase II. Reactions started with the addition of ATP to 1 mM. After incubation at 30°C, reactions were stopped by adding EDTA to 25 mM.

Electrophoretic Analysis of Knotted DNA. DNA samples were analyzed by electrophoresis in 0.4% agarose gels equilibrated with TBE buffer (100 mM Tris-borate, pH 8.3/2 mM EDTA). To facilitate manipulation, the gels were cast on top of a 2% agarose bed \approx 0.2 cm thick. After electrophoresis, gels were stained with ethidium bromide and destained with water. Ethidium-stained DNA was quantified with charge-coupled device technology by using a Fluor-S MultiImager system.

Monte Carlo Simulations. Knotting probabilities of equilateral polygons confined into spherical volumes were calculated by means of Markov-chain Monte Carlo simulations followed by rejection criteria. Freely jointed closed chains, composed of n equilateral segments, were confined inside spheres of fixed radius, r , and sampled: values of n ranged from 14 to 200 segments; r values, measured as multiples of the polygonal edge length, ranged from 2 to infinity. Excluded volume effects were not taken into account. Markov chains were generated by using the Metropolis algorithm (31). The temperature, a computational parameter, was held at $T = 300$ K to improve the efficiency of the sampling algorithm. Other values of T produced similar results, thus indicating that the computation is robust with respect to this parameter. Chains contained inside the sphere were assigned zero energy. Chains lying partly or totally outside the confining sphere were assigned an energy given by the maximum of the distances of the vertices of the chain to the origin. Only chains with zero energy were sampled. A random ensemble of polygons was generated by the crankshaft algorithm as follows: (i) two vertices of the chain were selected at random, dividing the polygon into two subchains, and (ii) one of the two subchains was selected at random (with equal probabilities for each subchain), and the selected subchain rotated through a random angle around the axis connecting the two vertices. This algorithm is known to generate an ergodic Markov chain in the set of polygons of fixed length (32). Correlation along the subchains was computed by using time-series analysis methods as described by Madras and Slade (33). Identification of the knotted polygons was achieved by computing the Alexander polynomial (14, 34) evaluated at $t = -1$ [denoted by $\Delta(-1)$]. It is known that $\Delta(-1)$ does not identify all knotted chains; however, for polygonal chains not confined to a spherical volume, nontrivial knots with trivial $\Delta(-1)$ values rarely occur. This circumstance has been observed by using knot invariants,

such as the HOMFLY polynomial, that distinguish between knotted and unknotted chains with higher accuracy than the Alexander polynomial. Our computer simulations (35) for small polygons (<55 segments) show that the knotting probabilities obtained by using $\Delta(-1)$ agree with those obtained by using the HOMFLY polynomial (32). Furthermore, Deguchi and Tsurusaki (36) have reported that the value of $\Delta(-1)$ can practically determine whether a given Gaussian polygon is trivial for lengths ranging from 30 to 2,400 segments (36).

Results

Knotting Probability of DNA Extracted from P4 Mature Phages, Capsids, and Tailless Mutants. The *E. coli* strain C-1895 was infected with P4 *vir1 del22*, and mature phages and capsids were purified from the bacterial lysate as described in *Materials and Methods*. Similarly, tailless mutants of P4 *vir1 del22* were prepared by infecting the *E. coli* strain C-8001 with higher titers of the P4 *vir1 del22* phage. DNA from the mature phages, capsids, and tailless mutants were extracted, avoiding treatments that would affect any preformed cohesive-end joining (28), and analyzed by agarose gel electrophoresis (Fig. 1A). One half of each sample was loaded directly in the gel, and the other half was heated at 75°C for 5 min and then chilled before gel loading. In the unheated samples (lanes 1, 3, and 5), three major forms of DNA were visible: linear monomers (L_1), unknotted circles (C_1), and a broad distribution of knotted circles (K). In the heated samples (lanes 2, 4, and 6), the transient disruption of cohesive ends converted most of the DNA knots to unknots and caused an increase in the monomeric (L_1) and multimeric forms of linear DNA (i.e., L_2). From these gel patterns, the amounts of linear monomers, unknotted circles, and knotted circles were calculated relative to the total DNA amount extracted from the mature phages, capsids, and tailless mutants. Fig. 1B summarizes these data. The relative amount of knotted DNA obtained was 0.47 for the mature phages, 0.88 for the capsids, and 0.95 for the tailless capsids. The spectrum of knot complexity was examined by scanning the distributions of knotted molecules and found to be very similar in the three kinds of phage particles, peaking at DNA knots of high crossing number. The relative amounts of knotted DNA obtained in the above experiments were not affected significantly by the method of DNA extraction. Extended incubation of tailless mutants with pancreatic DNase I or their treatment with 25 mM EDTA or 0.5% SDS before phenol extraction similarly yielded \approx 0.95 of highly knotted DNA molecules. We corroborated findings of previous studies (1, 29) that cyclization of linear P4 *vir1 del22* phage DNA in free solution (i.e., in phage buffer) has a knotting probability of \approx 0.03 and an average knot crossing number of less than 5 (data not shown).

Knot Complexity in DNA Extracted from P4 Tailless Mutants. Purified DNA from P4 *vir1 del22* tailless mutants was incubated with topoisomerase II as described in *Materials and Methods*. To examine the gradual removal of DNA knots by the topoisomerase, reactions were stopped after short time points, and the DNA samples examined by long-run gel electrophoresis (Fig. 2A). Catalytic amounts of topoisomerase II efficiently removed knots from circular DNA. The relative amount of unknotted circles (C) was 13% after 30 sec (lane 2) and 91% after 240 sec (lane 5). The progression of knot removal also resulted in the appearance of intermediate knots of low complexity, which were discernible as individual gel bands. Because the electrophoretic migration of knots formed on the same-size DNA molecules is related to the average crossing number of the ideal representation of the corresponding knot (37) and this relation is approximately linear up to knots with 10 crossings (38), populations of knots with 3, 4, 5, 6, 7, 8, 9, and 10 crossings were assigned to the distinguishable gel bands in Fig. 2A. Although it is known that some knots might deviate from this linear relation (39, 40), a

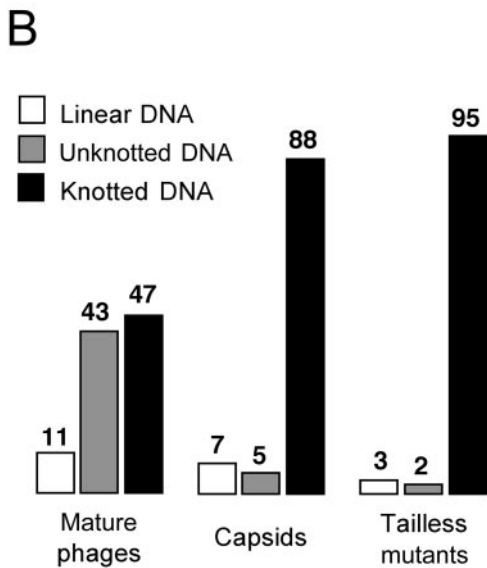
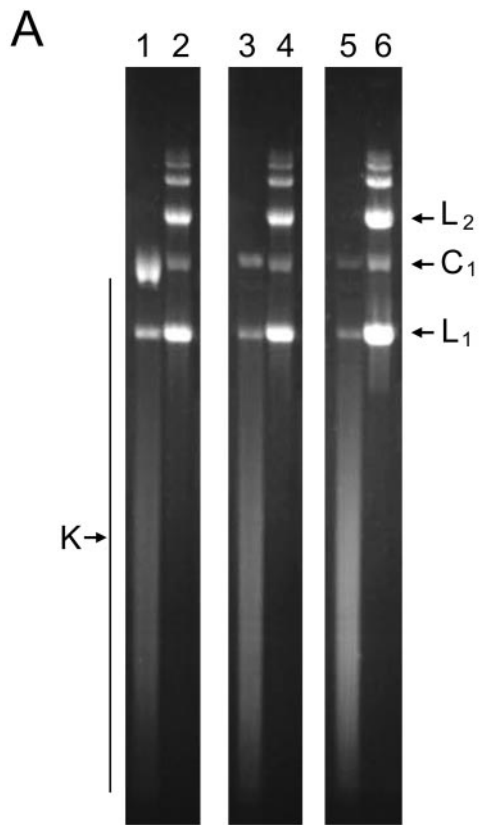


Fig. 1. Knotting probability of DNA extracted from different P4 phage particles. (A) Electrophoretic analysis of DNA extracted from P4 mature phages (lanes 1 and 2), P4 capsids (lanes 3 and 4), and P4 tailless mutants (lanes 5 and 6). In the odd lanes, purified DNA was loaded directly. In the even lanes, DNA was heated at 75°C for 5 min before loading in the gel. Electrophoresis was done in a 0.4% agarose gel and run at 35 V for 38 h. The positions of knotted DNA (K), linear monomers (L₁), linear dimers (L₂), and circular unknotted monomers (C₁) are indicated. (B) Relative amounts (%) of knotted, circular unknotted, and linear DNA extracted from mature phages, capsids, and tailless capsids.

continuous correlation between electrophoretic migration and the number of knot crossings also applies to more complex knots (41). Therefore, as a first approximation we used linear extrap-

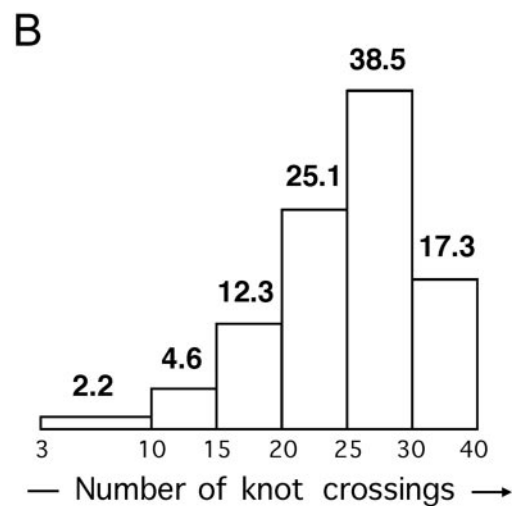
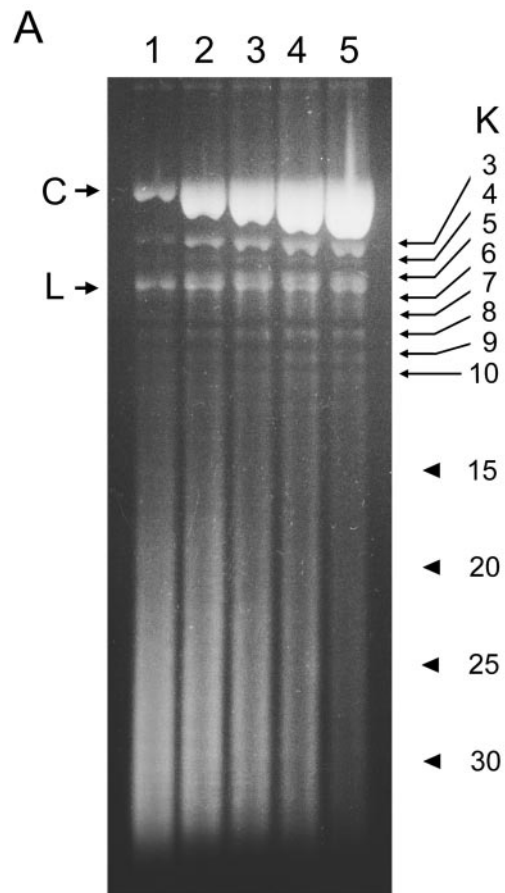


Fig. 2. Analysis of knot complexity in DNA molecules from P4 tailless mutants. (A) Time course unknottling of DNA by yeast topoisomerase II. Unknottling reactions were set as described in *Materials and Methods* and stopped at the following time points: 0 (lane 1), 30 (lane 2), 60 (lane 3), 120 (lane 4), and 240 sec (lane 5). These samples were electrophoresed in a 0.4% agarose gel that ran at 25 V for 45 h. The positions of linear DNA (L), unknotted circular DNA (C), and knotted circles (K) are indicated. Small arrows point to discernible bands of knotted circles with 3–10 crossings. Arrow heads point to the expected migration of knotted circles with 15, 20, 25, and 30 crossings, assuming a direct correlation between knot complexity and electrophoretic velocity. (B) Histogram of the knot complexity (number of crossings) of DNA extracted from P4 tailless mutants. The numbers at the top of each bar are percentages of the total amount of knotted molecules.

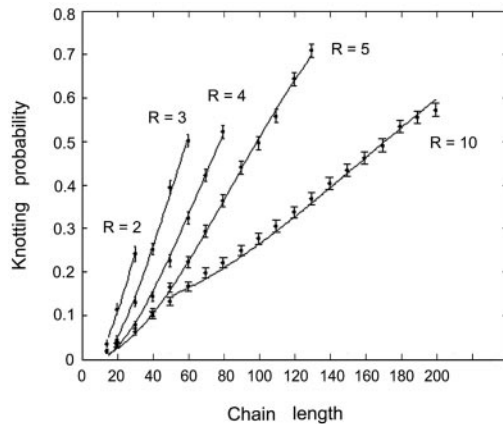


Fig. 3. Knotting probabilities of ideal equilateral chains confined to spheres of different radii as a function of the chain length. Chain lengths varied from 14 to 200 segments. Values of the radius (r), measured as the number of chain segments, of the confining sphere ranged from 2 to infinity. The figure shows the knotting probability for $r = 2, 3, 4, 5$, and 10. Error bars represent the SD for the observations made along the dynamic Markov chain (33).

olation to estimate the number of crossings of the more complex knot populations (Fig. 2B). Of the total amount of knotted molecules extracted from P4 tailless capsids, 2.2% had crossing numbers between 3 and 10, 4.6% had crossing numbers between 10 and 15, 12.3% had crossing numbers between 15 and 20, 25.1% had crossing numbers between 20 and 25, 38.5% had crossing numbers between 25 and 30, and 17.3% had crossing numbers greater than 30. The average number of knot crossings was ≈ 26.7 , and the largest number of knot crossings detected was ≈ 40 .

Monte Carlo Simulations of Knotting Probability. The effects of confinement of DNA molecules on DNA knotting probability was analyzed by Markov-chain Monte Carlo simulations (31). Symmetric Markov chains of freely jointed ideal equilateral polygons confined to spherical volumes were generated by importance sampling followed by rejection criteria as explained in *Materials and Methods*. From each of the selected polygons in the Markov chain a random projection was taken. From each regular projection the corresponding knot diagram (42) and its associated Dowker code (43) were computed and simplified (35) by removing crossings that did not change the knot type (Reidemeister I and II moves; ref. 42). On average, 75% of the crossings in each diagram were found to be removable without changing the knot type. Once the diagram was simplified, we computed its $\Delta(-1)$ value. Fig. 3 shows the knotting probability of closed ideal chains confined to spherical volumes of various radii (in multiples of edge length) as a function of the total chain length (number of edges in the equilateral polygon). Simulations performed for radii larger than the total chain length of the curve produced identical knotting results such as those obtained for simulations of freely jointed ideal chains of the same total length with no confinement (44). For a fixed confining volume that could contain polygons of various lengths, the knotting probability increased exponentially toward unity with polygon length. Similarly, knotting probabilities increased when polygons of constant lengths were confined to decreasing volumes. In addition, the complexity of the knots was measured by the average number of crossings of the simplified knot diagram. These results are summarized in Fig. 4. As expected, it was observed that for a fixed confining volume the complexity increased with the length of the polygon. For fixed length, the complexity decreased when the confining radius was increased.

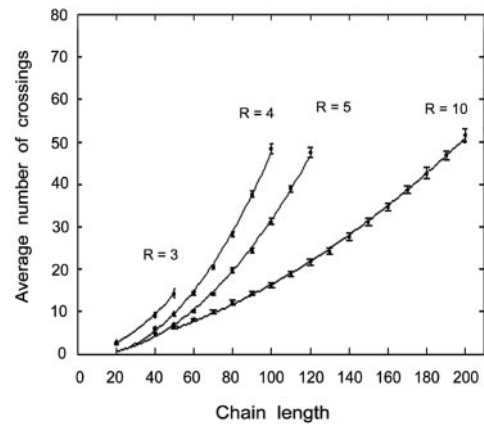


Fig. 4. Knot complexity of simplified diagrams as a function of chain length, measured as number of chain segments, in a confined volume of radius (r). The length of the chains varied from 20 to 200 segments. For each selected configuration the average number of crossings of the simplified diagrams, taken over 100 projections, was computed. This value is an upper bound for the crossing number of that configuration and approximates it. This process was repeated for all selected configurations along the Markov chain and averaged over the total number of analyzed configurations. The figure shows the variation of knot complexity (average number of crossings) for $r = 3, 4, 5$, and 10. Error bars were computed by using methods from time-series analysis (33).

Discussion

Experimental and theoretical studies of knotting of double-stranded DNA molecules in free solution have shown that the knotting probability of a 10-kb DNA molecule that undergoes random cyclization in a solvent containing 10 mM $MgCl_2$ is ≈ 0.03 (1, 29). Both experimental and simulation data show that the major knotted result of such random cyclization is the 3-crossing (trefoil) knot and that minor products are knots with 4 and 5 crossings. These values are in sharp contrast with the high knotting probability values found in the experimental and simulation results reported here. For P4 *vir1 del22* mature phages, DNA knotting probability was 0.47, which is higher than reported previously (10). For P4 *vir1 del22* capsids and tailless mutants, DNA knotting probabilities were 0.88 and 0.95, respectively. In addition, the three kinds of phage particles were found to have similar very high knot complexities as well. Over 97% of the knots in tailless mutants had more than 10 crossings; assuming a close linear correlation between knot complexity and electrophoretic velocity, the average number of knot crossings along the knot spectrum was estimated to be ≈ 26.7 .

What are the factors that could affect the formation of knots so dramatically? It is highly unlikely that the DNA sequence itself could promote such high knotting values. It has been observed experimentally that the knotting probability of P4 DNA molecules in free solution coincides with the probability predicted by computer simulations for general DNA molecules of the same length and effective diameter (5). This result argues against the existence of intrinsic bends of the P4 DNA that could favor the formation of knots. Another possibility is that knotting could be promoted by physical interactions between the DNA and viral capsid or between different segments of the DNA molecule inside the capsid. Nevertheless, there is experimental evidence showing that at least 98% of the DNA packed in bacteriophages retains its B form, with only small perturbations in the base stacking (45). Also, the absence of specific interactions between any region of the viral DNA and the capsid or within regions of the DNA molecule has been inferred from cross-linking experiments (46, 47). Therefore, we suggest that the major factor contributing to the high probability of DNA

knotting is the confinement of DNA inside the viral capsid. Consistent with this hypothesis, our Monte Carlo simulations, corroborating previous studies (14, 15, 32), reveal that confinement of DNA chains in restricted volumes causes a large increase in knotting probability. We found that the knotting probability and knot complexity vary directly with chain length for fixed confining radius and inversely with confining radius for fixed chain length. This correlation indicates that for cyclization reactions in confined volumes, confinement plays a major role in the formation of the knots by increasing both the probability and complexity of the observed knots.

Cyclization of DNA inside the P4 phage particles is possible provided that both cohesive ends of the linear DNA have enough freedom to find each other. Yet, in mature phage particles one end of the viral DNA is known to be anchored near the tail-connector region (19, 20). This anchoring obstructs the cyclization of DNA inside the capsid. Nonetheless, we found that almost 50% of the DNA molecules extracted from mature phages are knotted. The origin of these knots can be attributed to either of the following two scenarios. In the first scenario, the anchored end of the DNA gets loose in a significant fraction of phages, and cyclization takes place inside the capsid. Such an event might be caused by imperfect morphogenesis or by phage decline during experimental manipulation. In the second scenario, the linear DNA is released in free solution from the phage particle and rapidly becomes cyclic in partial volume confinement before it reaches entropic equilibrium as a free linear chain. This cyclization would still trap some of the geometric packing complexity of the confined DNA, giving rise to large knotting probabilities and complexity.

In contrast, the knotting probability of DNA extracted from capsids and tailless mutants is almost double that from mature phages. Independent of the procedure used to disrupt the phage particles, less than 5% of the DNA molecules extracted from tailless mutants were unknotted. The same DNA-knotting sce-

narios described above for mature phages could be considered here. Yet, judging from the mature phage results and assuming that the knots were formed outside the phage particle, it can be calculated that at least 48% of the DNA extracted from tailless mutants must become end-joined inside the phage particle. This assessment is consistent with the fact that extended DNase treatment of the tailless mutants had no effect on knotting probability and complexity, which indicated that neither end of the DNA is accessible from outside the phage particle before extraction. Therefore, we conclude that at least half the knotted molecules obtained from capsids and tailless mutants must result from random cyclization of the DNA inside the capsid and that, consequently, neither of the DNA ends is likely to be anchored inside such particles.

Our experimental and simulated results show that complicated knotting might be a general feature relevant to the common situation of highly confined DNA loops, yet this finding does not discard other factors that could affect knotting probability and distribution further such as the packing configuration of DNA or the volume exclusion of DNA. Simulations of polygons with volume exclusion in confined volumes should help uncover other structural features not examined in this study.

We thank R. Calendar for providing material for preparing P4 phages and J. C. Wang, A. Stasiak, S. G. Whittington, and R. K. Sachs for helpful discussions and comments on the manuscript. We also thank S. G. Whittington for making available to us the program for calculating autocorrelation times and statistical errors for dynamic Markov chains. We are grateful to Mr. Carles Rojals for his assistance during phage and DNA preparation. J.A. and M.V. were supported by the Program in Mathematics and Molecular Biology through a Burroughs Wellcome Fund Interfaces Grant and by National Science Foundation Grant DMS-9971169. M.V. was supported by a Dirección General de Asuntos del Personal Académico-Universidad Nacional Autónoma de México graduate fellowship. This research was supported also by Ministry of Science of Spain Grant PB98-0487.

- Rybenkov, V. V., Cozzarelli, N. R. & Vologodskii, A. V. (1993) *Proc. Natl. Acad. Sci. USA* **90**, 5307–5311.
- Shaw, S. Y. & Wang, J. C. (1993) *Science* **260**, 533–536.
- Wasserman, S. A. & Cozzarelli, N. R. (1986) *Science* **232**, 951–960.
- Stark, W. M., Boocock, M. R. & Sherratt, D. J. (1989) *Trends Genet.* **5**, 304–309.
- Frank-Kamenetskii, M. D., Lukashin, A. V., Anshelevich, V. V. & Vologodskii, A. V. (1985) *J. Biomol. Struct. Dyn.* **2**, 1005–1012.
- Schlick, T. & Olson, W. K. (1992) *Science* **257**, 1110–1115.
- Tesi, M. C., Janse van Resburg, E. J., Orlandini, E., Sumners, D. W. & Whittington, S. G. (1994) *Phys. Rev. E Stat. Phys. Plasmas Fluids Relat. Interdiscip. Top.* **49**, 868–892.
- Sumners, D. W. (1990) *Math Intelligencer* **12**, 71–80.
- Shishido, K., Komiya, N. & Ikawa, S. (1987) *J. Mol. Biol.* **195**, 215–218.
- Liu, L. F., Davis, J. L. & Calendar, R. (1981) *Nucleic Acids Res.* **9**, 3979–3989.
- Liu, L. F., Perkocha, L., Calendar, R. & Wang, J. C. (1981) *Proc. Natl. Acad. Sci. USA* **78**, 5498–5502.
- Ménissier, J., de Murcia, G., Lebeurier, G. & Hirth, L. (1983) *EMBO J.* **2**, 1067–1071.
- Mansfield, M. L. (1994) *Macromolecules* **27**, 5924–5926.
- Michels, J. P. J. & Wiegel, F. W. (1986) *Proc. R. Soc. London Ser. A* **403**, 269–284.
- Tesi, M. C., Janse van Resburg, J., Orlandini, E. & Whittington, S. G. (1994) *J. Phys. A Math. Gen.* **27**, 347–360.
- Lindqvist, B. H., Deho, G. & Calendar, R. (1993) *Microbiol. Rev.* **57**, 683–702.
- Wang, J. C., Martin, K. V. & Calendar, R. (1973) *Biochemistry* **12**, 2119–2123.
- Rishoud, S., Holzenburg, A., Johansen, B. V. & Lindqvist, B. H. (1998) *Virology* **245**, 11–17.
- Chattoraj, D. K. & Inman, R. B. (1974) *J. Mol. Biol.* **87**, 11–22.
- Casjens, S. (1997) *Structural Biology of Viruses*, eds. Chiu W., Burnett R. & Garcea R. (Oxford Univ. Press, Oxford), pp. 3–37.
- Black, L. W., Newcomb, W. W., Boring, J. W. & Brown, J. C. (1985) *Proc. Natl. Acad. Sci. USA* **82**, 7960–7964.
- Cerritelli, M. E., Cheng, N., Rosenberg, A. H., McPherson, C. E., Booy, F. P. & Steven, A. C. (1997) *Cell* **91**, 271–280.
- Earnshaw, W. C. & Harrison, S. C. (1977) *Nature (London)* **268**, 598–602.
- Hud, N. (1995) *Biophys. J.* **69**, 1355–1362.
- Lepault, J., Dubochet, J., Baschong, W. & Kellenberger, E. (1987) *EMBO J.* **6**, 1507–1512.
- Wolfson, J. S., McHugh, G. L., Hooper, D. C. & Schwartz, M. N. (1985) *Nucleic Acids Res.* **25**, 6695–6702.
- Raimondi, A., Donghi, R., Montaguti, A., Pessina, A. & Deho, G. (1985) *J. Virol.* **54**, 233–235.
- Isaksen, M., Julien, B., Calendar, R. & Lindqvist, B. H. (1999) *DNA Topoisomerase Protocols, DNA Topology, and Enzymes*, eds. Bjornsti M. A. & Osheroff N. (Humana, Totowa, NJ), Vol. 94.
- Rybenkov, V. V., Ullsperger, C., Vologodskii, A. V. & Cozzarelli, N. R. (1997) *Science* **277**, 690–693.
- Worland, P. J. & Wang, J. C. (1989) *J. Biol. Chem.* **264**, 4412–4416.
- Metropolis, N., Rosenbluth, A. W., Rosenbluth, M. N., Teller, A. H. & Teller, E. (1953) *J. Chem. Phys.* **21**, 1087–1092.
- Millet, K. (1994) in *Series of knots and everything*, eds. Sumners D. W. & Millett K. C. (World Scientific, Singapore), Vol. 7, pp. 31–46.
- Madras, N. & Slade, G. (1993) in *The Self-Avoiding Walk* (Birkhäuser, Boston).
- Frank-Kamenetskii, M. D., Lukashin A. V. & Vologodskii, A. V. (1975) *Nature (London)* **258**, 398–402.
- Arsuaga, J. (2000) Ph.D. thesis (Florida State Univ., Tallahassee, FL).
- Deguchi, T. & Tsurusaki, K. (1994) *J. Knot Theor. Ramifactions* **3**, 321–353.
- Katrich, V., Bednar, J., Michoud, D., Dubochet, J. & Stasiak, A. (1996) *Nature (London)* **384**, 142–145.
- Vologodskii, A., Crisona, N. J., Laurie, B., Pieranski, P., Katritch, V., Dubochet, J. & Stasiak, A. (1998) *J. Mol. Biol.* **278**, 1–3.
- Cantarella, J., Kusner, R. B. & Sullivan, J. M. (1998) *Nature (London)* **392**, 237–238.
- Buck, G. (1998) *Nature (London)* **392**, 238–239.
- Spengler, S. J., Stasiak, A. & Cozzarelli, N. R. (1985) *Cell* **42**, 325–334.
- Burde, G. & Zieschang, H. (1985) *Knots* (de Gruyter, Berlin), Vol. 5.
- Dowker, C. H. & Thistlethwaite, M. B. (1983) *Topology Appl.* **16**, 19–31.
- Vologodskii, A. (1992) *Topology and Physics of DNA* (CRC, Boca Raton, FL).
- Aubrey, K. L., Casjens, S. R. & Thomas, G. J., Jr. (1992) *Biochemistry* **31**, 11835–11842.
- Haas, R., Murphy, R. P. & Cantor, C. R. (1982) *J. Mol. Biol.* **159**, 71–92.
- Serwer, P., Hayes, S. J. & Watson, R. H. (1992) *J. Mol. Biol.* **223**, 999–1011.